Optimal Linear Control of Modular Multi-Level Converters with a Prescribed Degree of Stability

Elyas Rakhshani, Kumars Rouzbehi, Juan Manuel Escaño & Jose Rueda Torres

Published online: 26 Mar 2020.

Submit your article to this journal ⬈

Article views: 108

View related articles ⬈

View Crossmark data ⬈

Taylor & Francis
Taylor & Francis Group

🔓 OPEN ACCESS   Check for updates

Optimal Linear Control of Modular Multi-Level Converters with a Prescribed Degree of Stability

Elyas Rakhshani [iD],[1] Kumars Rouzbehi [iD],[2] Juan Manuel Escaño [iD],[2] and Jose Rueda Torres [iD][1]

[1]Department of Electrical Sustainable Energy, Delft University of Technology (TU Delft), Delft, the Netherlands
[2]Departamento de Ingeniería de Sistemas y Automática, University of Seville, Seville, Spain

CONTENTS

Abstract—In this paper, a new control approach using an optimal linear control with prescribed degree of stability for modular multi-level converters (MMC) is presented and analyzed. The proposed controller relies on a linear quadratic regulator with integral action which brings the ability of state variable reference tracking for modular multi-level converters. Since MMC is a complex system with several state variables, a unified control system design for this system is vital. The proposed controller of this study is designed to obtain wider stability margin thanks to the implementation of prescribed degree of stability concept to minimize the quadratic performance index of the control structure. By means of this method, the poles of the closed-loop system will be shifted to the desired places in the left half side of the S-plane. The main advantages of this control strategy compared to previous methods are that it will be possible to control the state of energy for each phase separately, while there will be superior tolerance to nonlinearities and the enhanced stability margin with less sensitivity to plant-parameter variations. The performance of the designed controller is verified through MATLAB$^{\text{TM}}$ simulations (The MathWorks, Natick, MA, USA) with the nonlinear model of MMC.

1. INTRODUCTION

The main features of modern power electronic converters are their ability to establish sinusoidal waveforms on their AC side with lowest amounts of harmonics, much lower switching losses, flexibility to extend to high voltage/power ratings, reliability to faults, etc. [1]. Toward these objectives, the first report on multi-level converters was published in 1975 [2]. Three-level converter was the first type of multi-level converters family [3]. Following this brilliant advancement, in the next years, several topologies for multi-level power converters were introduced [4, 5]. So far, between various topologies of multi-level power converters, the modular multi-level converters (MMC) seems to be the most promising solution for wide power range applications [6–9]. Actually, this type of power converter

was first introduced by A. Lesnicar and R. Marquardt [6], and later Saeedifard and Iravani [4] have established an MMC-based back-to-back HVDC system and they showed its merits under unbalanced grid conditions. The modularity of this converter topology brings more reliability during transient operation, and by increasing the numbers of cells, different levels of voltage can be achieved [7–11]. However, the control complexity due to increase of the MMC state variables is still a challenging topic [12]. One of the main control challenges for these types of converters is insuring that the capacitor voltage (or stored energy) is properly controlled to obtain the required output voltage level in the AC side and [8, 13]. As the number of modules increases, the number of the state variables that should be controlled will increase. In this case, conventional controllers will be faced to a huge complexity. Since, the total number of all the state variables in the MMC that need a proper control is significant, a transition from conventional control approaches to advanced control techniques seems to be more promising [14].

The applications of robust controllers and sliding mode control approaches are reported in different research papers [15–18]. The main use of these methods is their advantages on simplicity and robustness [17, 18]. A predictive control, based on minimizing a cost function, has been used for balancing the capacitor voltages and to minimize the circulating currents of the MMC [19]. Since MMC is a MIMO system, different state variables should be controlled in a proper manner. At the same time, each controller should be simple and easy for the sake of implementation. In this regard, linear quadratic regulator (LQR) as an optimal control technique can become a suitable candidate to control such a modular power converter [20]. As reported in [21–23], LQR approach with the integral action with tracking ability is appropriate for MIMO systems and its satisfactory performance for various applications is demonstrated.

As the main contribution of this paper, a new approach based on an extension of LQR method with a prescribed degree of stability is presented and analyzed. In the proposed control approach, it is possible to control the energy of each phase independently, which will bring more reliability to the converter operation. In the case of several cells, for balancing the energy of each cell, the difference in the energy of the cell with respect to its portion of the total energy in the leg will be considered as the state. Therefore, it is possible to control the energy of each cell as well. However, to provide wider margins of stability to LQR controller, prescribed degree of stability is added to the system. The main advantage of this strategy is that
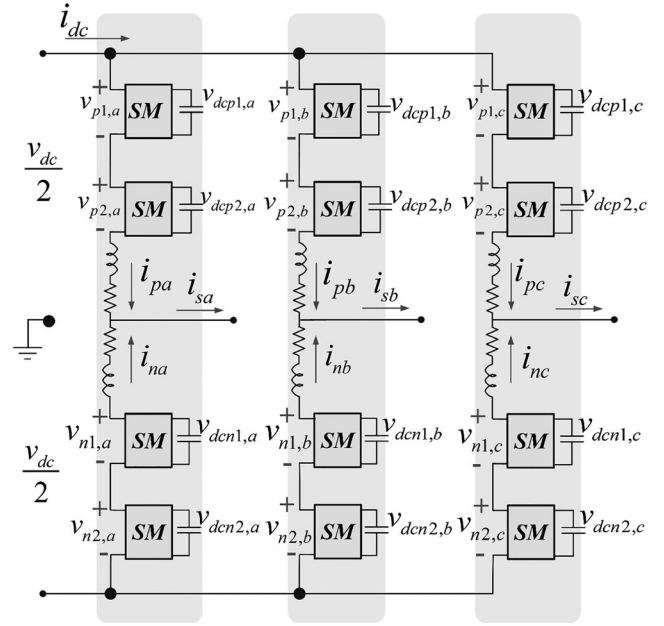

FIGURE 1. General structure of MMC in three-phase with two cells.

there will be a higher tolerance and enhanced stability margin with less sensitivity to plant-parameter variations. The proposed method can be easily extended to the MMC with more cells. The performance and eligibilities of the proposed controller are verified through MATLAB simulations with the nonlinear model of MMC. The simulation results show that the proposed method satisfies MMC control criterions, with a satisfactory dynamic response.

The rest of the paper is structured as the following. In Section 2, mathematical presentation of the three-phase MMC considering the AC current and energy balancing control is reported. Later, in Section 3, the proposed optimal controller with a prescribed degree of stability is designed and presented. System analysis and simulation results validating the proposed control approach for the nonlinear MMC are presented and discussed in Section 4, and finally, the paper is concluded in Section 5.

2. MATHEMATICAL MODEL OF MMC

As shown in Figure 1, one MMC consists of series-connected identical modules per phase called sub-modules or cells. The string of this series of sub-modules is called a leg of converter. Each leg is divided into upper and lower arms such that the number of sub-modules of each arm is identical. The mid-point between each arm serves as the AC phase connection point. Inductors are placed between each arm to achieve filtering requirements and to limit

transient currents between each arm. Each sub-module may be made up of different types of topologies with energy storage capacitors. The basic operation principle of the converter is inserting or bypassing the charged capacitors in each sub-module arm to create a voltage difference between each arm, which is the output voltage of the converter.

An average-based model is selected in this paper [5, 8]. The mathematical presentation in this study is used for extracting a suitable state space model which will be essential for designing a suitable LQR controller. Referring to Figure 1, four cells per leg are selected. (two of the cells are in the upper arm, and two more cells are in the lower arm).

The main equations presenting the dynamic behavior of MMC are categorized as the current control equations and the energy balancing control equations. The linearized presentations of these equations are as follows.

2.1. Modeling of Current Controllers

The equations representing the AC currents and circulating current are the main equations in this part. Based on the equations, it is clear that the output AC current (i_s), injected to the gird, is the addition of the upper current (i_p) and the lower (i_n) arm current (Eq. (1)), while the circulating current (i_c) is assumed as half of the difference between the upper current and the lower arm current (Eqs. (2) and (3)).

$$i_s = i_p + i_n \tag{1}$$

$$i_d = i_p - i_n \tag{2}$$

$$i_c = \frac{i_d}{2} = \frac{i_p - i_n}{2} \tag{3}$$

After a dq transformation, the equations of three-phase system for AC currents can be as follows:

$$\frac{d}{dt}\begin{bmatrix} i_{s,a} \\ i_{s,b} \\ i_{s,c} \end{bmatrix} = -\frac{R}{L}\begin{bmatrix} i_{s,a} \\ i_{s,b} \\ i_{s,c} \end{bmatrix} - \frac{1}{L}\begin{bmatrix} v_{e-ac,a} \\ v_{e-ac,b} \\ v_{e-ac,c} \end{bmatrix} - \frac{2}{L}\begin{bmatrix} v_{s,a} \\ v_{s,b} \\ v_{s,c} \end{bmatrix} \tag{4}$$

Using the park transformation, the AC current equations can be presented in dq-frame like this:

$$\frac{d}{dt}\begin{bmatrix} i_{s,d} \\ i_{s,q} \end{bmatrix} = \begin{bmatrix} \frac{-R}{L} & \omega \\ -\omega & \frac{-R}{L} \end{bmatrix}\begin{bmatrix} i_{s,d} \\ i_{s,q} \end{bmatrix} - \frac{1}{L}\begin{bmatrix} v_{e-ac,d} \\ v_{e-ac,q} \end{bmatrix} - \frac{2}{L}\begin{bmatrix} v_{s,d} \\ v_{s,q} \end{bmatrix} \tag{5}$$

Therefore, as explained the circulating current or differential currents can be calculated as follows:

$$\frac{d}{dt}i_{d,a} = -\frac{R}{L}i_{d,a} - \frac{1}{L}v_{i,a} + \frac{1}{L}V_{DC} \tag{6}$$

$$\frac{d}{dt}i_{d,b} = -\frac{R}{L}i_{d,b} - \frac{1}{L}v_{i,b} + \frac{1}{L}V_{DC} \tag{7}$$

$$\frac{d}{dt}i_{d,c} = -\frac{R}{L}i_{d,c} - \frac{1}{L}v_{i,c} + \frac{1}{L}V_{DC} \tag{8}$$

while v_{e-ac} is the AC component of the external control signal or the AC current control equations and v_i is the internal control signal with its 100-Hz frequency.

$$v_p - v_n = v_e = v_{e-AC} + v_{\Delta e-DC} \tag{9}$$

$$v_p + v_n = v_i \tag{10}$$

Therefore, a new DC component is considered in Eq. (9) which will be another control signal ($v_{\Delta e-DC}$). This control signal will be applied for presenting the equations related to the balancing of energies among the upper and the lower arms.

2.2. Modeling of Modules Energy

In this section, all the related equations presenting the energy behavior of each sub-module of MMC are presented. Each sub-module is modeled as an equivalent voltage source. The energies of sub-modules are used as separated state variables which will be presented in the state space model. This state space model is used for designing the LQR controller for MMC control.

2.2.1. Balancing of Total Energy. One of the most advantageous points of the control approach designed in this work is its ability to have three independent controls over the energy state in each phase separated from each other. This capability of the controller can provide more reliability in the operation of MMC especially during defective and transient conditions. The total energy in the MMC will be the sum of the upper arm and the lower arm quantities. Therefore, the equation of total energy that will be implemented in control design procedure can be written as follows:

$$e_t = \int P_{dcp}(t) + P_{dcn}(t)dt \tag{11}$$

where P_{dcp} and P_{dcn} are the power of upper and lower arms, separately. This equation can be rewritten based on upper and lower currents, i_s and i_d, which will represent part of the state space equations of our MM model:

$$\frac{d}{dt}e_t = v_p i_p - v_n i_n = v_p\left(\frac{i_s}{2} + \frac{i_d}{2}\right) - v_n\left(\frac{i_s}{2} - \frac{i_d}{2}\right) \tag{12}$$

$$\frac{d}{dt}e_t = \frac{i_s}{2}(v_p - v_n) + \frac{i_d}{2}(v_p + v_n) \tag{13}$$

$$\frac{d}{dt}e_t = \frac{i_s}{2}\ v_e + \frac{i_d}{2}\ v_i \tag{14}$$

It is worthy to mention that for the controller design step, the average value of Eq. (12) is considered.

2.2.2. Differential Energy Balancing.

To guaranty the balance of DC voltage or energy among the upper arm and the lower arm, the following equation as the differential energy balancing equations are considered. For obtaining the following equations, the differences between the energy of the upper arm and the lower arm can be defined in terms of arms' power:

$$e_d = \int P_{dcp}(t) + P_{dcn}(t)dt \tag{15}$$

The same as before, the differential energy equations can be rewritten based on the AC currents and differential currents:

$$\frac{d}{dt}e_d = v_p i_p + v_n i_n = v_p\left(\frac{i_s}{2} + \frac{i_d}{2}\right) + v_n\left(\frac{i_s}{2} - \frac{i_d}{2}\right) \tag{16}$$

$$\frac{d}{dt}e_d = \frac{i_s}{2}\ (v_p + v_n) + \frac{i_d}{2}\ (v_p - v_n) \tag{17}$$

$$\frac{d}{dt}e_d = \frac{i_s}{2}\ v_i + \frac{i_d}{2}v_e \tag{18}$$

2.2.3. Module Balancing.

Another objective of a full controlled system is the control of the energy state of each cell of the MMC. For doing this control action, the difference in the energy of modules with respect to its portion of the total energy in each leg can be considered as new state. Therefore, for several cells (here, the number of cells is N), $N-1$ additional control signal with new states will be defined for each leg. Based on this explanation, the module balancing equation for the upper arm is as follows:

$$v_{p-j} = \frac{v_p}{N} + \Delta v_{p-j}\ \ , j = 1 : N \tag{19}$$

where, $\Delta v_{\Delta p-j}$ is a new DC control signal which is responsible for controlling the energy change in each module and $\sum_j \Delta \dot{e}_{p-j} = 0$. For the equation of lower arm, the same approach will result in the following equation:

$$v_{n-j} = \frac{v_n}{N} + \Delta v_{n-j}\ \ , j = 1 : N \tag{20}$$

The average value for these new states will be used for the global state space system.

Finally, a proper linearization around the operating point of the model can lead to its suitable equations for designing the LQR controller. The procedure for designing and validations of the designed controller is explained and discussed in the following sections. Therefore, it can be assumed that the states of a nonlinear MMC system, named $(x(t))$, can have a small change $(\hat{x}(t))$ around its rating operational point value (X):

$$x(t) = \hat{x} + X \tag{21}$$

Then, considering the previous clarification, we can obtain the state space model as follows:

$$\dot{x} = Ax + Bu \tag{22}$$

3. CONTROLLER DESIGN

3.1. Linear Quadratic Regulator

The LQR is a well-known strategy of optimal control. During the design of LQR, to regulate the states of the linear time-invariant model presented by Eq. (22), the following control law can be used to control the system as MIMO model

$$u = -K\ x \tag{23}$$

To minimize the following cost function

$$J = \int_0^\infty (x^T Q x + u^T R u)dt \tag{24}$$

where R is the weighting matrix of the control action and Q the weighting of the state. Q is a positive-semi-definite matrix and R is a positive-definite matrix. Substituting Eq. (23) into Eq. (22), we obtain

$$\dot{x} = Ax - BKx = (A - BK)x \tag{25}$$

It is well known [24] that the system is stable (or $A - BK$ is stable), if

$$K = R^{-1}B^T P \tag{26}$$

and P is a positive-definite matrix that satisfies the reduced-matrix Riccati equation $A^T P + PA - PBR^{-1}B^T P + Q = 0$.

In the state space model of the MMC, there are some states that need to be tracked and controlled to some specific values as reference. For doing this, one supplementary integral controller will be added. Therefore, the new state space matrices considering these new integral actions are shown as follows:

$$A_I = \begin{bmatrix} A & 0 \\ C1 & 0 \end{bmatrix}\ B_I = \begin{bmatrix} B \\ 0 \end{bmatrix}$$

$$B_{Idis} = \begin{bmatrix} B_{dis} \\ 0 \end{bmatrix}\ C1_I = \begin{bmatrix} C1 & 0 \end{bmatrix} \tag{27}$$

Therefore, a new output matrix will be selected in a way that those specific states that should be tracked can be considered in the feedback:
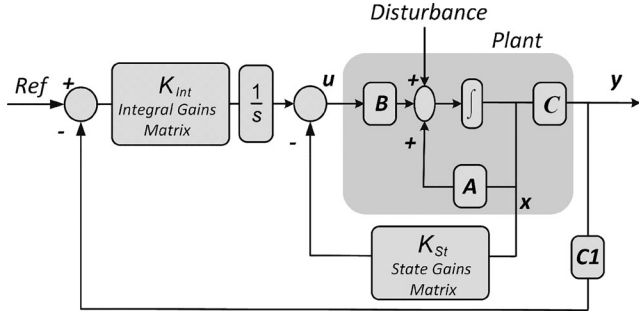
FIGURE 2. Equivalent control diagram of the LQR with an integral action controller.

$$x_{aug} = \left[\hat{x} \ \left| \int \hat{x} \right] \right. \text{ and } y_1 = C1_I x_1$$

For this augmented state space system, a new control law will be considered as follows:

$$u_I = (R - y_1)\frac{K_i}{s} - K_{states}x \qquad (28)$$

Later, the new equations of the augmented LQR controller with integral actions can be modified for designing the controller gains:

$$A_I^T P + P A_I - P B_I R^{-1} B_I^T P + Q = 0 \qquad (29)$$

$$K_{aug} = R^{-1} B_I^T P \qquad (30)$$

In the control design stage, the general control structure of the LQR with an integral action is presented in Figure 2, where the linear state space model of the MMC will be used to design the proper controller. Later, with adding two interfaces, the controller will be test with averaged model of MMC.

For example for the MMC with one cell in each arm, we have $K_{aug}(4 \times 9)$ that is the total augmented matrix gains which is optimally calculated. This matrix gain should be divided into two parts like the proportional matrix (K_{states} (4×5)) and the integral action matrix (K_i (4×4)) as follows:

$$K_{aug} = \begin{pmatrix} K_{11} & K_{12} & K_{13} & K_{14} & K_{15} & K_{16} & K_{17} & K_{18} & K_{19} \\ K_{21} & K_{22} & K_{23} & K_{24} & K_{25} & K_{26} & K_{27} & K_{28} & K_{29} \\ K_{31} & K_{32} & K_{33} & K_{34} & K_{35} & K_{36} & K_{37} & K_{38} & K_{39} \\ K_{41} & K_{42} & K_{43} & K_{44} & K_{45} & K_{46} & K_{47} & K_{48} & K_{49} \end{pmatrix}$$

$$K_{states} = \begin{pmatrix} K_{11} & K_{12} & K_{13} & K_{14} & K_{15} \\ K_{21} & K_{22} & K_{23} & K_{24} & K_{25} \\ K_{31} & K_{32} & K_{33} & K_{34} & K_{35} \\ K_{41} & K_{42} & K_{43} & K_{44} & K_{45} \end{pmatrix},$$

$$K_i = \begin{pmatrix} K_{16} & K_{17} & K_{18} & K_{19} \\ K_{26} & K_{27} & K_{28} & K_{29} \\ K_{36} & K_3 & K_{38} & K_{39} \\ K_{46} & K_{47} & K_{48} & K_{49} \end{pmatrix}$$

$$(31)$$

As a result, the proper objective function will be considered like in Eq. (32):

$$J = \int_0^\infty (x_I^T Q x_I + u^T R u)dt = \int (J_x + J_u)dt \qquad (32)$$

Therefore, the weighting factors for the MMC with one cell will be calculated as follows:

$$Q = \begin{bmatrix} Q_{sd} & 0 & 0 & 0 & 0 & 0 & 0 & 0 & 0 \\ 0 & Q_{sq} & 0 & 0 & 0 & 0 & 0 & 0 & 0 \\ 0 & 0 & Q_z & 0 & 0 & 0 & 0 & 0 & 0 \\ 0 & 0 & 0 & Q_{\dot{w}} & 0 & 0 & 0 & 0 & 0 \\ 0 & 0 & 0 & 0 & Q_{\Delta\dot{w}} & 0 & 0 & 0 & 0 \\ 0 & 0 & 0 & 0 & 0 & Q_{\int i_{sd}} & 0 & 0 & 0 \\ 0 & 0 & 0 & 0 & 0 & 0 & Q_{\int i_{sq}} & 0 & 0 \\ 0 & 0 & 0 & 0 & 0 & 0 & 0 & Q_{\int \dot{w}} & 0 \\ 0 & 0 & 0 & 0 & 0 & 0 & 0 & 0 & Q_{\int \Delta\dot{w}} \end{bmatrix},$$

$$R = R_w \cdot \begin{bmatrix} 1 & 0 & 0 & 0 \\ 0 & 1 & 0 & 0 \\ 0 & 0 & 1 & 0 \\ 0 & 0 & 0 & 1 \end{bmatrix}$$

The performance index J in Eq. (32) which consists of integral sum of the performance criterion J_x and the control efforts J_u can be presented as follows:

$$J_x = Q_{sd}(\hat{i}_{sd})^2 + Q_{sq}(\hat{i}_{sq})^2 + Q_z(\bar{\hat{i}}_z)^2 + Q_{\dot{w}}(\bar{\hat{w}})^2$$

$$+ Q_{\Delta\dot{w}}(\Delta\bar{\hat{w}})^2 + Q_{\int i_{sd}}\left(\int \hat{i}_{sd}\right)^2 + Q_{\int iq}\left(\int \hat{i}_{sq}\right)^2$$

$$+ Q_{\int \dot{w}}\left(\int \bar{\hat{w}}\right)^2 + Q_{\int \Delta\dot{w}}\left(\int \Delta\bar{\hat{w}}\right)^2 J_u$$

$$= R_w\left[(\hat{v}_{macd})^2 + (\hat{v}_{macq})^2 + (\hat{v}_{mdc})^2 + (\hat{v}_{\Delta w})^2\right] \qquad (33)$$

The designed values for weights should be calculated based on the following points:

- Getting the fastest dynamic response without deteriorating effects.
- Avoiding of saturation in any of the control variables.

3.2. Linear Controller with Prescribed Degree of Stability

A new modified quadratic function for the system of Eq. (22) can be defined which leads to a linear control law of the type represented in Eq. (23), with some added characteristics that the closed-loop system poles can be lied to the left side of $Re(s) = -\alpha$, $\alpha > 0$, in the s-plane [14, 25].

The performance index in Eq. (32) is modified by the one presented in Eq. (38):

$$J_o = \int_{t_0}^\infty e^{\alpha t}[x^T(t)Qx(t) + u^T(t)Ru(t)]dt \qquad (38)$$

While in this new performance index, the parameter α will be a constant value that can be chosen by designer and design criterions. The same as previous definitions, R and Q are also the positive definite symmetric and non-negative definite symmetric constants, respectively. Then, for minimizing Eq. (38) subject to the conditions presented by Eq. (22), set:

$$\hat{x}(t) = e^{\alpha t}.x \ , \ \hat{u} = e^{\alpha t}.u \tag{39}$$

While Eq. (22) should be equivalent to Eq. (40):

$$\dot{\hat{x}}(t) = (A + \alpha I_n)x.(t) + B.\hat{u}(t), \ \hat{x}(t_0) = e^{\alpha t_0}.x_0 \tag{40}$$

Considering $(u^T R.u + x^T Q.x).e^{\alpha t} = \hat{u}^T.R.\hat{u} + \hat{x}^T.Q.\hat{x}$, and hence, minimization with respect to Eq. (22) of Eq. (38) will be equivalent to the minimization with respect to Eq. (40) of the following:

$$J_o = \int_{t_0}^{\infty} (\hat{x}^T(t).Q.\hat{x}(t) + \hat{u}^T(t).R.\hat{u}(t)) \tag{41}$$

Considering that:

a. The minimum of Eq. (38) (stated in terms of x_0) will be the same as the minimum of the Eq. (41) (stated in terms of $\hat{x}(t_0)$, taking into account that $\hat{x}(t_0) = e^{\alpha t_0}.x_0$].

b. If the optimal control for Eqs. (40) and (41) is $\hat{u} = f(x)$, accordingly $u = e^{-\alpha t}f(xe^{\alpha t})$ will be the optimal control for Eqs. (22) and (38), and conversely.

The first remark here is not as significant as the second one; it is clear that, for Eqs. (43) and (44), the optimal control will be

$$\hat{u}(t) = -K_\alpha \hat{x}(t) \tag{42}$$

where

$$K_\alpha = R^{-1}B^T P_\alpha \tag{43}$$

and P_α will be the unique non-negative definite solution of the following modified Riccati equation:

$$(A + \alpha I_n)^T P_\alpha + P_\alpha(A + \alpha I_n) - P_\alpha B R^{-1} B^T P_\alpha + Q = 0 \tag{44}$$

3.2.1. Stability of the Closed-loop System.
Usually, closed-loop linear systems have to be stable. Consequently, the design of the optimal control law has to lead to an asymptotically stable system as well. This can be explained as follows:

For the system of Eqs. (22)–(24), let H be any matrix so that $Q = HH'$, and let (A, H) be completely observable (i.e., $H'e^{AT}a = 0$ for all t implies $a = 0$). Then, the closed-loop system is asymptotically stable. (Besides, P is positive definite.)

Clearly, this is an important result. However, it fails to yield any measure of stability. The closed-loop poles are in
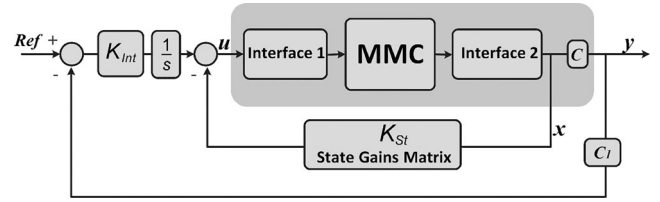

FIGURE 3. General control structure.

the left half of the s-plane, but how far they are from the imaginary axis is not known. In Section 3.2, of course, we seek to put a minimum distance between the closed-loop poles and the imaginary axis.

The requirement of complete observability is vital in the following sense; if Eq. (22) have unstable states which are not observable, then precisely because these states do not affect the performance index (Eq. (24)), there will be no control action trying to stabilize these states. Accordingly, the closed loop will be unstable. In the event that unobservable states are all asymptotically stable, one can, however, rely on the closed-loop system being asymptotically stable too.

Now, let us consider the closed-loop poles of the $\dot{x} = (A - BK_\alpha)x$. We shall assume, as before, that with H any matrix such that $HH' = Q$, the pair (A, H) is completely observable. Then, the system defined by Eqs. (39) and (42) is surely asymptotically stable, as indicated in Section 3.1. This system is $\dot{\hat{x}} = (A - BK_\alpha + \alpha I)\hat{x}$, and since the poles of this system, being given by the eigenvalues of $A - BK_\alpha + \alpha I$ have negative real parts, it follows that the poles of $\dot{x} = (A - BK'_x)x$, being given by the eigenvalues of $A - BK'_\alpha$ (which are less by $\propto$ than the eigenvalues of $(A - BK'_\alpha + \alpha I)$), all possess real parts less than $-\alpha$.

It is worthy to mention that the main benefit of the proposed control with prescribed degree of stability in comparison with the conventional optimal regulator will be the reduction of system's sensitivity to the plant parameter changes [25]. This robustness, as results in a closed-loop control, is bigger for $\alpha > 0$ than for $\alpha = 0$.

3.2.2. Controller Implementation.
The LQR gives a multivariable proportional regulator, and it would be essential to add an integrator in the controller for eliminating the steady-state errors between the reference signals and the controlled state variable, which in this case is the AC current and the energy variations. In other words, the LQR control must have integral action. The complete block diagram of one LQR with the integral action for averaged MMC and two additional interfaces is shown in Figure 3.
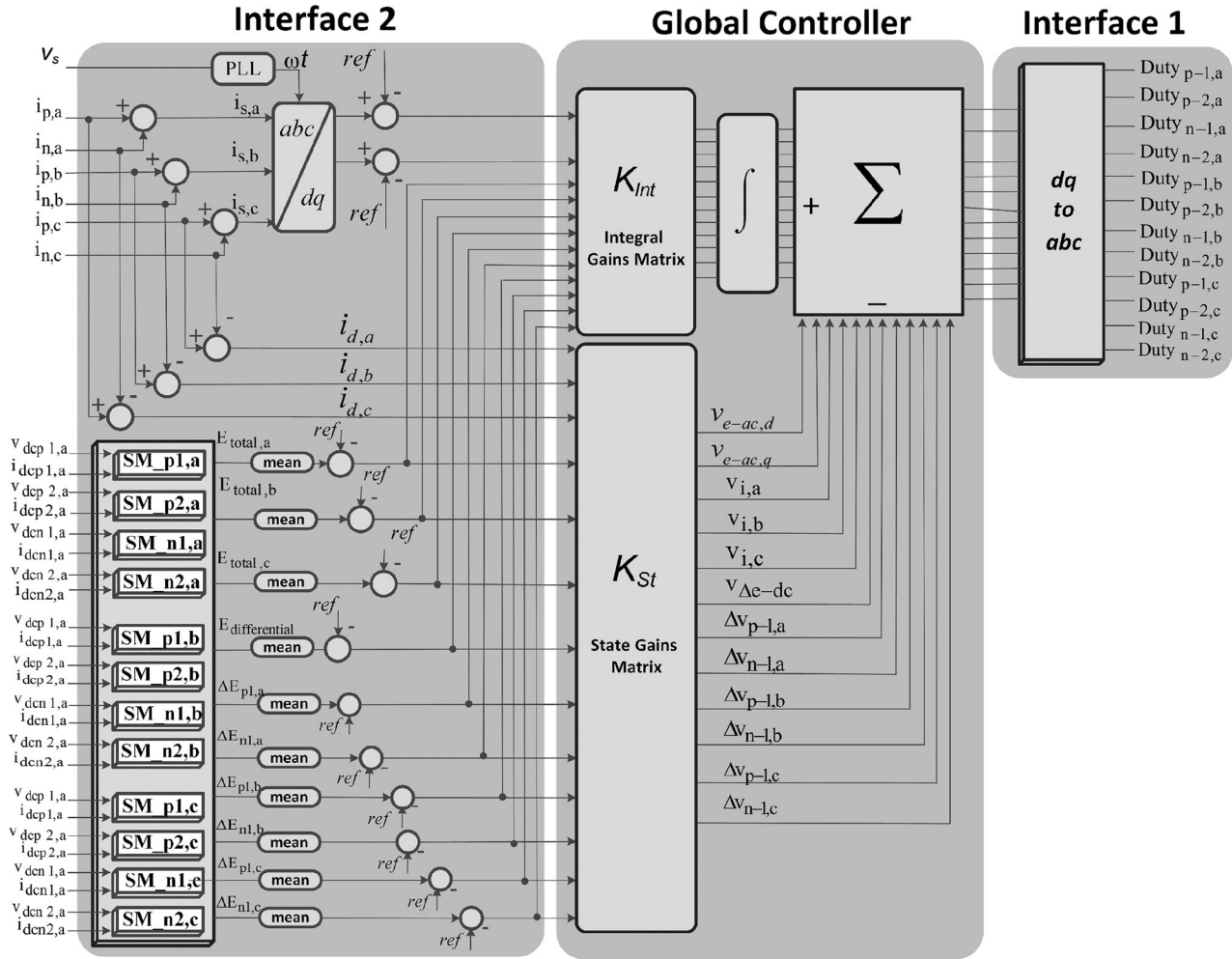
FIGURE 4. Detailed of controller implementation for LQR with integral action.

Detailed controller diagram are presented in Figure 4. Based on this figure, for implementing the controller we used two interfaces, one for using the calculated state for feedback (interface1) and the other interface for using the output of controller for calculating the duty cycles as input of plant (interface2). To evaluate this controller, we have implemented it for nonlinear model of MMC in Simscape Power Systems^{TM} (The MathWorks, Natick, MA, USA).

4. SYSTEM ANALYSIS

4.1. Sensitivity Analysis

In this section, to show the validity and acceptable performance of the designed linear controller for modular converter, simulation is performed using a nonlinear model of modular converter in Simscape Power Systems^{TM}. In other word, the designed controller based on linear equations is

tested for control and energy balancing of a nonlinear MMC model. The parameters used for this study case is presented in Table 1.

According to the presented information in Table 2, a case study for testing the performance of the controller on tracking various step changes in different working conditions is performed. Therefore, different step changes on the input references of the systems are introduced. The main proposed action of this test is to assess the validity of the proposed linear model in the three-phase MMC.

According to Figure 5, the tracking and control performance for the *dq* components of the AC current is depicted. It was assumed that after 0.5 sec, the AC reference current is changing to 2 (A) for injection to the grid.

As shown in these figures, the dynamics of controller for tracking the current is very fast and is able to track the reference changes in less than 0.012 sec. Figure 6 is also showing the ability of the designed controller on tracking

Parameters	Value
R	40 $m\Omega$
L	2.5 mH
v_s	100 V
R_{load}	50 Ω
C per module	3300 μF
V_{DC}	700 V
N per arm	2
f_s	50 Hz

TABLE 1. Converter parameters for the base case study.

| Reference changes	Time (s)	Value
AC current	0.5	2 A
Total Energy-Phase A	1	50 J
Total Energy-Phase B	1.5	35 J
Total Energy-Phase C	2	20 J
Total Energy-Phase A	9.4	−50 J
Total Energy-Phase B	9.6	−35 J
Total Energy-Phase C	9.8	−20 J
Energy of each individual modules	5.5	23.42
Energy of each individual modules	7	− 23.42

TABLE 2. Reference values for the general studied case.

the step changes of energy state references for each phase of the multi-modular converter. It shows that after changing the AC current reference at 0.5 sec the energy states in each phase, after a short dynamics, remain the same as before.

It is clear that during injection of AC current, usually the stored energy of the capacitors will start to decrease and after a short time the controller is trying to compensate it for maintaining the balance between AC and DC power exchange.

The three-phase shape of the injected AC current is also depicted in Figure 7(a). As shown in this figure, the current is totally balanced and completely matched with the chosen reference input (2A).

Also, one comparison among the upper and lower arm currents of the MMC is also presented in Figure 7(b). It can be seen that the arm currents they have a DC component while the total AC current which is injected to the grid will be a pure AC signal. By the following figures, Figures 8(a)–8(c), the response of the capacitor voltages considering those different changes in the energy references can be followed. Firstly, as shown in Table 2, total energy of each phase is increasing separately and after that (as shown in Figure 8(a)), for checking the ability of the controller to follow the reference change for each individual module, the references point for each module are changing at 5.5 and 7 sec (Figure 8(b)). Finally, as
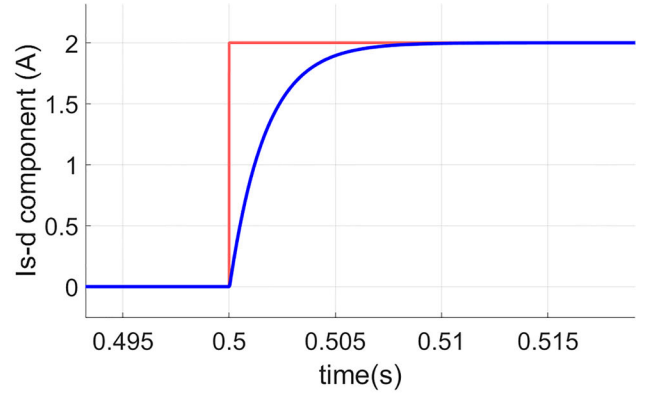
(a)
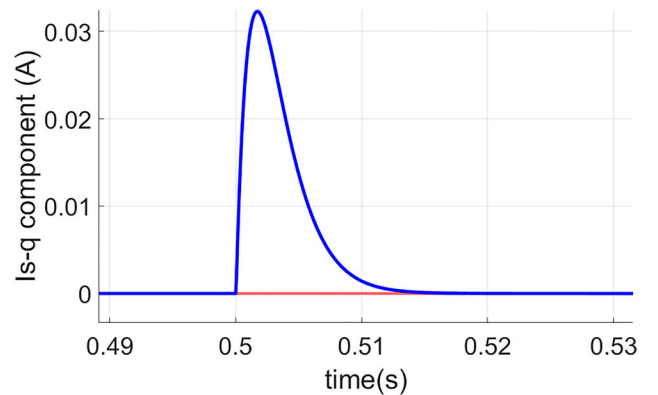
(b)

FIGURE 5. Responses of dq component for the injected AC current (I_{sd}, I_{sq}). (a) d-component and (b) q-component.
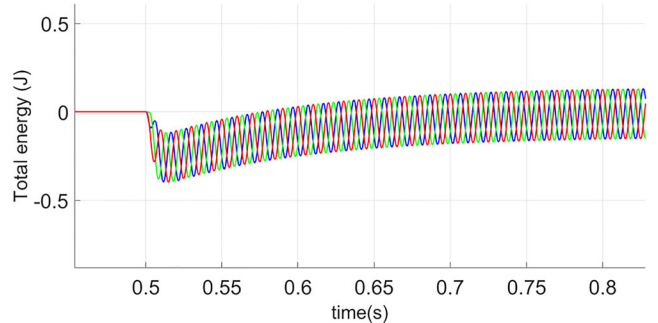
FIGURE 6. Energy-balancing change (in phases a, b and c) after AC current injection at $t = 0.5$ sec.

presented in Figure 8(c), based on the orders coming from the references, the controller is able to force all the energies coming come back to their initial reference points.

Therefore, based on the performed case study, the performance and the capability of the proposed controller for different types of contingency are tested.
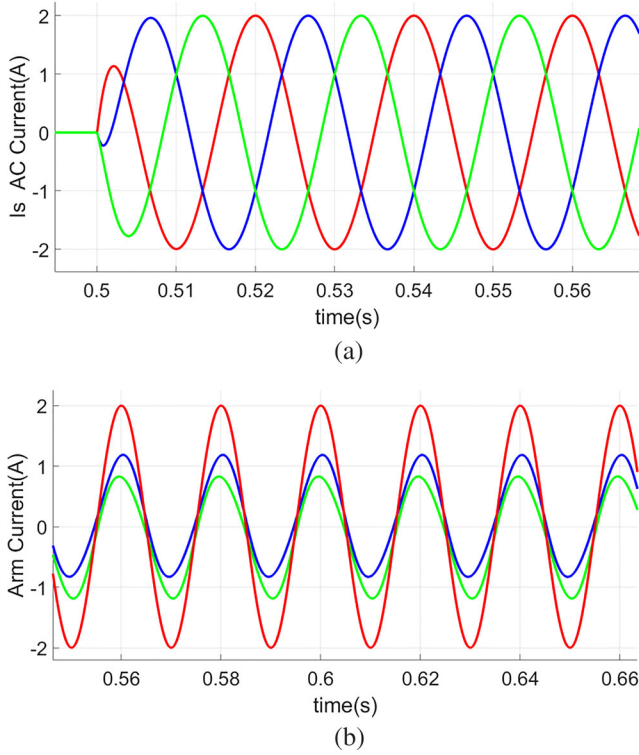
FIGURE 7. Injected currents: (a) three-phase AC current and (b) arm currents. (Red trace: AC current I_s, Blue trace: Upper arm current I_p and Green trace: Lower arm I_n).

4.2. Analysis with Parameter Variations

In this section, for validating the performance of the controller with the proposed control based on prescribed degree of stability against the parameter variations, the simulations are repeated under significant change of plant parameter from their rating values. These new values are presented in Table 3. It should be note that plant response under these selected values for parameters is oscillatory and more close to stability limits. Therefore, in this way it would be easier to compare and to see the effect of prescribed degree of stability control for improving the system performance during parameter changes.

For this case study, first we design a normal LQR with integral action for the MMC, and then as a second step, the modified controller based on the prescribed degree of stability will be implemented. As explained before, the feedback control law of Eq. (22) is modified by Eqs. (41)–(44) and it will be used for the system with the prescribed degree of stability. It is assumed that in this simulation, the value of α constant is equal to 15.

Simulation results for the system with normal LQR controller are presented in Figures (5)–(8). These results show the ability of designed LQR for controlling the MMC.
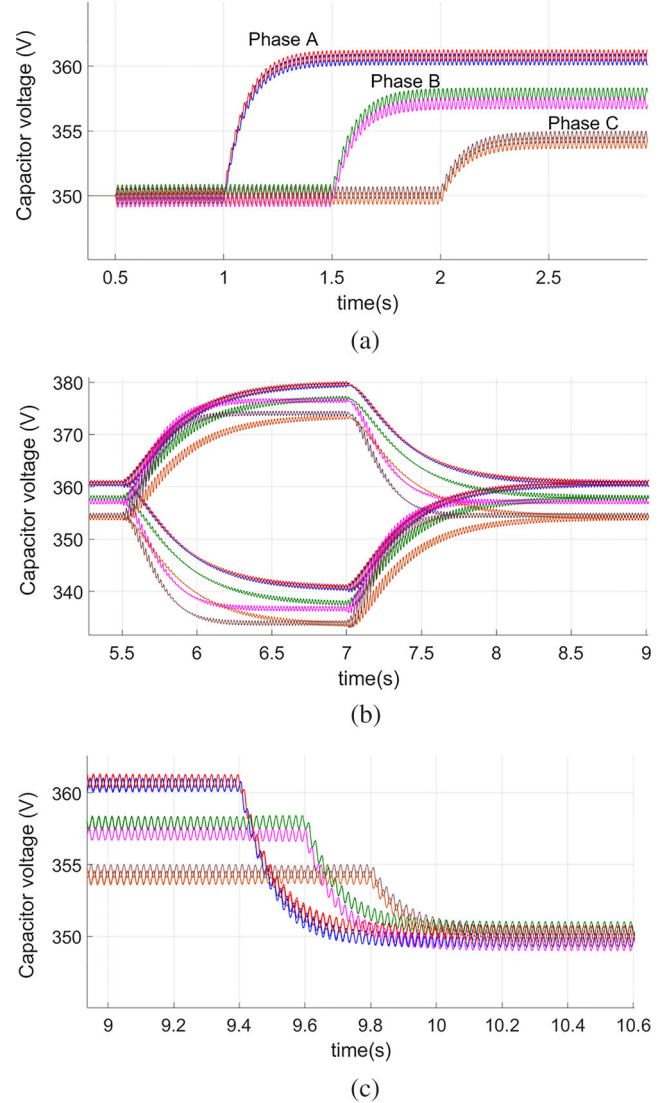

FIGURE 8. Energy states for different modules of MMC: (a) an increase in the voltage of capacitors (energy) for

Parameters	Value
R	10 mΩ
L	20 mH
v_s	100 V
C per module	3300 μF
V_{DC}	700 V
N per arm	2
f_s	50 Hz

TABLE 3. Parameter of MMC for second case.

As it was explained, the prescribed degree of stability concept is added to the LQR controller for more improvement in the dynamic performance and eigenvalues of the
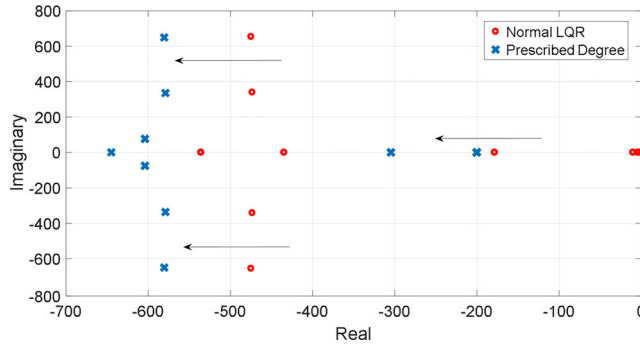
FIGURE 9. Eigenvalues of the system: with (a) the normal LQR controller and with (b) the proposed control approach.

| Eigenvalues	LQR	LQR-Prescribed
1	$-474 + j654$	$-580 + j649$
2	$-474 - j654$	$-580 - j649$
3	$-473 + j340$	$-579 + j335$
4	$-473 - j340$	$-579 - j335$
5	-434.77	-644.89
6	-434.77	$-603 + j763$
7	-434.77	$-603 - j763$
8	-535.63	$-603 + j763$
9	-535.91	$-603 - j763$
10	-535.90	$-603 + j763$
11	-535.90	$-603 - j763$
12	-10.300	-304.60
13	-4.000	-304.61
14	-4.360	-304.63
15	-4.360	-304.63
16	-10.20	-304.63
17	-10.20	-304.63
18	-2.450	-200.53
19	-2.450	-200.08
20	-178.50	-200.09
21	-178.50	-200.10
22	-178.53	-200.52
23	-178.53	-200.52
24	-178.53	-200.03
25	-178.53	-200.03
26	-2.450	-200.03
27	-2.450	-200.03

TABLE 4. Parameter values of MMC for simulated case.

system. As shown in Figure 9 and Table 4, after implementing the proposed control, the eigenvalues of the system can shifted to the left side of the s plane for having a better performance.

Another comparison is presented in Figures 10(a) and 10(b), for the controls with and without prescribed degree of stability. Based on the results, it is clear that the system with normal LQR shows a higher peak of overshoot, but
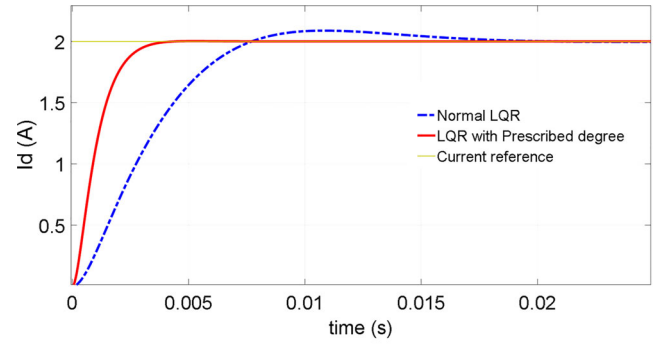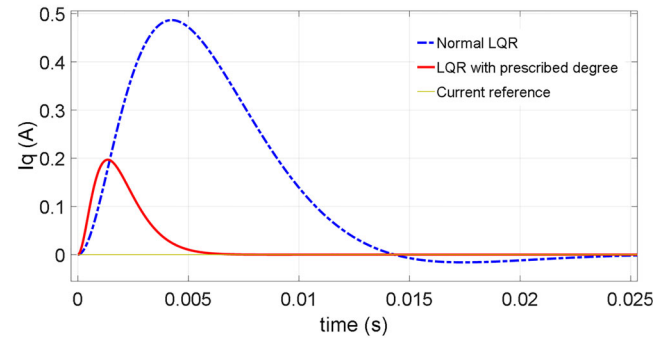
FIGURE 10. Current components: (a) d component of injected current in dq frame for second case study and (b) q component of injected current in dq frame for second case study.

by adding the proposed control concept significant improvement in the dynamic response of the system will be accessible when overshoot and time response could be improved, thus being tested the robustness of the proposed strategy.

5. CONCLUSION

In this study, a new control design for a systemic modeling and control of three-phase MMCs which is based on the state space equations and optimal linear quadratic control was presented and discussed. This control method is implemented to an average-based MMC model and a complete set of equations to design a suitable LQR with an integral action is presented. To improve the overall system stability, the concept of prescribed degree of stability is introduced by modifying its regular LQR controller to obtain decent dynamic response. Finally, the proposed controller is assessed and verified through the developed simulation platform. Results show that the system speed is increased, at the same time the dynamic oscillations are rapidly damped out and the system's sensitivity to the plant-parameter variations is significantly reduced.

ORCID

Elyas Rakhshani ⓘ http://orcid.org/0000-0002-6463-4251
Kumars Rouzbehi ⓘ http://orcid.org/0000-0002-3623-4840
Juan Manuel Escaño ⓘ http://orcid.org/0000-0003-1274-566X
Jose Rueda Torres ⓘ http://orcid.org/0000-0001-7288-0228

REFERENCES

[1] K. Rouzbehi, S. S. Heidary, and N. Shariati, "Power flow control in multi-terminal HVDC grids using a serial-parallel DC power flow controller," *IEEE Access*, vol. 6, pp. 56934–56944, 2018. DOI: 10.1109/ACCESS.2018.2870943.

[2] R. H. Baker and L. H. Bannister, "Electric power converter," U.S. Patent number: 3,867,643, filled on January 14, 1974.

[3] A. Nabae, I. Takahashi, and H. Akagi, "A new neutral-point clamped PWM inverter," *IEEE Trans. Ind. Appl.*, vol. IA-17, no. 5, pp. 518–523, 1981. DOI: 10.1109/TIA.1981.4503992.

[4] M. Saeedifard and R. Iravani, "Dynamic performance of a modular multilevel back-to-back HVDC system," *IEEE Trans. Power Delivery*, vol. 25, no. 4, pp. 2903–2912, 2010. DOI: 10.1109/TPWRD.2010.2050787.

[5] E. Sánchez-Sánchez, E. Prieto-Araujo, A. Junyent-Ferré, and O. Gomis-Bellmunt, "Analysis of MMC energy-based control structures for VSC-HVDC links," *IEEE J. Emerging Select. Topics Power Electron.*, vol. 6, no. 3, pp. 1065–1076, Sept. 2018. DOI: 10.1109/JESTPE.2018.2803136.

[6] A. Lesnicar and R. Marquardt, "An innovative modular multilevel converter topology suitable for a wide power range," Power Tech Conference 2003, Bologna, Italy, Jun. 23–26, 2003.

[7] L. Harnefors, A. Antonopoulos, S. Norrga, L. Angquist, and H.-P. Nee, "Dynamic analysis of modular multilevel converters," *IEEE Trans. Ind. Electron.*, vol. 60, no. 7, pp. 2526–2537, 2012. DOI: 10.1109/TIE.2012.2194974.

[8] J. Lyu, X. Zhang, X. Cai, and M. Molinas, "Harmonic state-space based small-signal impedance modeling of a modular multilevel converter with consideration of internal harmonic dynamics," *IEEE Trans. Power Electron.*, vol. 34, no. 3, pp. 2134–2148, 2019. DOI: 10.1109/TPEL.2018.2842682.

[9] K. Rouzbehi, J. Zhu, W. Zhang, G. B. Gharehpetian, A. Luna, and P. Rodriguez, "Generalized voltage droop control with the inertia mimicry capability - step towards automation of multi-terminal HVDC grid," Proc. International Conference on Renewable Energy Research and Application (ICRERA), Palermo, Italy, Nov. 22–25, 2015.

[10] S. Yang, Y. Tang, and P. Wang, "Distributed control for a modular multilevel converter," *IEEE Trans. Power Electron.*, vol. 33, no. 7, pp. 5578–5591, 2018. DOI: 10.1109/TPEL.2017.2751254.

[11] B. Gutierrez and S.-S. Kwak, "Modular multilevel converters (MMCs) controlled by model predictive control with reduced calculation burden," *IEEE Trans. Power Electron.*, vol. 33, no. 11, pp. 9176–9187, 2018. DOI: 10.1109/TPEL.2018.2789455.

[12] G. Bergna-Diaz, J. Are Suul, and S. D'Arco, "Energy-based state-space representation of modular multilevel converters with a constant equilibrium point in steady-state operation," *IEEE Trans. Power Electron.*, vol. 33, no. 6, pp. 4832–4851, 2018. DOI: 10.1109/TPEL.2017.2727496.

[13] F. Zhang and J. X. C. Zhao, "New control strategy of decoupling the AC/DC voltage Offset for modular multi-level converter," *IET Gener. Transm. Distrib.*, vol. 10, no. 6, pp. 1382–1392, 2016. DOI: 10.1049/iet-gtd.2015.0797.

[14] K. Rouzbehi and E. Rakhshani, "An ICA based multi-objective optimization for VSC-HVDC stations control in multi-terminal HVDC grids," *Electric Power Compon. Syst.*, vol. 47, no. 4–5, pp. 316–328, 2016. DOI: 10.1080/15325008.2019.1608479.

[15] M. Belhaouane, M. Ayari, X. Guillaud, and N. Benhadj Braiek, "Robust control design of MMC-HVDC systems using multivariable optimal guaranteed cost approach," *IEEE Trans. Ind. Appl.*, vol. 55, no. 3, pp. 2952–2963, 2019. DOI: 10.1109/TIA.2019.2900606.

[16] H. R. Baghaee, M. Mirsalim, G. B. Gharehpetian, and H. A. Talebi, "Decentralized sliding mode control of WG/PV/FC microgrids under unbalanced and nonlinear load conditions for on- and off-grid modes," *IEEE Syst. J.*, vol. 12, no. 4, pp. 3108–3119, Dec. 2018. DOI: 10.1109/JSYST.2017.2761792.

[17] E. Rakhshani, A. M. Cantarellas, D. Remon, P. Rodriguez, and I. Candela, "Modeling and control of multi modular converters using optimal LQR controller with integral action," 2013 IEEE Energy Conversion Congress and Exposition, Denver, CO, Sept. 15–19, 2013, pp. 3965–3970.

[18] Q. Yang, M. Saeedifard, and M. A. Perez, "Sliding mode control of the modular multilevel converter," *IEEE Trans. Ind. Electron.*, vol. 66, no. 2, pp. 887–897, Feb. 2019.

[19] J. Qin and M. Saeedifard, "Predictive control of a modular multilevel converter for a back-to-back HVDC system," *IEEE Trans. Power Deliv.*, vol. 27, pp. 1538–1547, 2012. DOI: 10.1109/TPWRD.2012.2191577.

[20] C. Olalla, R. Leyva, A. El Aroudi, and I. Queinnec, "Robust LQR control for PWM converters: An LMI approach," *IEEE Trans. Ind. Electron.*, vol. 56, no. 7, pp. 2548–2558, Jul. 2009. DOI: 10.1109/TIE.2009.2017556.

[21] B. Kedjar and K. Al-Haddad, "DSP-based implementation of an LQR with integral action for a three-phase three-wire shunt active power filter," *IEEE Trans. Ind. Electron.*, vol. 56, no. 8, pp. 2821–2828, 2009. DOI: 10.1109/TIE.2008.2006027.

[22] R. Salim, H. Y. Kanaan, K. Al-Haddad, and B. Khedjar, "LQR with integral action controller applied to a three-phase three-switch three-level AC/DC converter," 36th Annual Conference on IEEE Industrial Electronics Society IECON 2010, Glendale, AZ, Nov. 7–10, 2010, pp. 550–555.

[23] O. S. Ebrahim, M. F. Salem, P. K. Jain, and M. A. Badr, "Application of linear quadratic regulator theory to the stator field-oriented control of induction motors," *IET Electric Power Appl.*, vol. 4, no. 8, pp. 637–646, 2010. DOI: 10.1049/iet-epa.2009.0164.

[24] K. Ogata, *Modern Control Engineering: International Edition*, 5th ed. USA: Pearson Higher Ed., 2009.

[25] B. K. Kumar, S. N. Singh, and S. C. Srivastava, "A decentralized nonlinear feedback controller with prescribed degree of stability for damping power system oscillations," *Electric Power Syst. Res.*, vol. 77, no. 3–4, pp. 204–211, 2007. DOI: 10.1016/j.epsr.2006.02.014.

BIOGRAPHIES

Elyas Rakhshani received his PhD (cum laude), in electrical engineering from Technical University of Catalonia (UPC), Barcelona, Spain, in 2016. From 2013 to 2016, he joined ABENGOA Company, Seville, Spain, as a junior researcher, working on different projects related to power electronics applications and the flexible operation of modern power systems. Since 2017, he is working as a Postdoctoral Researcher at the Delft University of Technology (TU Delft) with IEGP Research Center, the Netherlands. He joined IEPG center since the beginning of 2017 working on European H2020 projects related to control and dynamic stability assessment of low-inertia renewable-based power systems. Based on his research, he published and presented several scientific works/papers in the most distinguished journals and international conferences in electrical engineering. His research interests are power system control and dynamic stability; HVDC control and power converter applications in power systems; wind power integration, frequency control, and optimal intelligent control.

Kumars Rouzbehi received the PhD degree in electric energy systems from the Technical University of Catalonia (UPC), Barcelona, Spain. Prior to this, he was with the faculty of Electrical Engineering as academic staff, Islamic Azad University, from 2004 to 2011. In parallel with teaching and research at the IAU, he was the CEO of Khorasan Electric and Electronics Industries Researches Company from 2004 to 2010. From 2017 to 2019, he was an associate professor at the Loyola Andalucía University, Seville, Spain. In 2019, he joined the Department of Systems and Automatic Engineering, University of Seville, Spain. He holds one patent and has authored/coauthored more than 70 technical books, journal and conference papers. Dr. Rouzbehi is serving as an Associate Editor in IET Renewable Power Generation, IET High Voltage, and IET Energy Systems Integration since 2018. His research interests include control of power converters, renewable energy, energy storage, HVDC transmission systems.

Juan Manuel Escaño received his PhD in control engineering from the University of Seville, in 2015. He is a Research Fellow at the University of Seville, a senior member of IEEE, a member of IFAC, ISA and a member and coordinator of the Fuzzy Control working group of EUSFLAT. He has been an associate professor at the Loyola Andalucía University (Seville, Spain), leader of the Advanced Control Systems Group at the Nimbus Center at the Cork Institute of Technology (Cork, Ireland) and Advanced Process Control Engineer for Air Products and Chemistry (Europe). He has more than 30 years of experience in academia and industry, participating in different research projects in the process and energy industry. He has coauthored more than 60 scientific and technical publications with several articles in national and international conferences. His research interests are intelligent control systems, fuzzy model predictive control, embedded control systems and fault detection.

José L. Rueda Torres was born in 1980. He received the PhD in electrical engineering from the Universidad Nacional de San Juan, San Juan, Argentina, in 2009. From 2003 to 2005, he worked in Ecuador, in the fields of industrial control systems and electrical distribution networks operation and planning. Between 2010 and 2014, he was a Postdoctoral Research Associate with the Institute of Electrical Power Systems, University of Duisburg-Essen, Essen, Germany, where he is currently pursuing the 'Habilitation' (qualification) postdoctoral degree. Currently, he is an Associate Professor for Intelligent Electrical Power Grids in the Department of Electrical Sustainable Energy, Technical University, Delft, the Netherlands. Dr. Rueda is Vice-Chair of the Working Group on Modern Heuristic Optimization under the IEEE PES Power System Analysis, Computing, and Economics Committee. His research interests include power system stability and control, system identification, power system planning, as well as probabilistic and artificial intelligence methods.